

## DOPPLER SHIFT OSCILLATIONS OF HOT SOLAR CORONAL PLASMA SEEN BY SUMER: A SIGNATURE OF LOOP OSCILLATIONS?

TONGJIANG WANG, S. K. SOLANKI, W. CURDT, D. E. INNES, AND I. E. DAMMASCH  
Max-Planck-Institut für Aeronomie, Postfach 20, D-37191 Katlenburg-Lindau, Germany; wangtj@linmpi.mpg.de  
Received 2002 April 24; accepted 2002 June 5; published 2002 June 24

### ABSTRACT

We report observations of strongly damped Doppler shift oscillations detected in a flare line, Fe XIX, with the Solar Ultraviolet Measurement of Emitted Radiation spectrometer. Spectra were recorded above an active region at the western limb of the Sun, from lines with formation temperatures ranging from 0.01 to 10 MK. However, the oscillations were seen only in the hot plasma ( $>6$  MK) lines. The Doppler oscillations have periods of 14–18 minutes, with an exponential decay time of 12–19 minutes, and show an initial large blueshift pulse with peak velocities up to  $77 \text{ km s}^{-1}$ . Several indications suggest that the Doppler oscillations are incompressible coronal loop oscillations that are excited impulsively by a flarelike event that also produced a strong increase in Fe XIX emission.

*Subject headings:* Sun: corona — Sun: flares — Sun: UV radiation — Sun: X-rays, gamma rays

### 1. INTRODUCTION

Previous reports on oscillations of the coronal plasma are mainly based on quasi-periodic patterns observed in modulated radio emission (see Aschwanden 1987) and propagating disturbances in EUV emission (e.g., Berghmans & Clette 1999). These observations have been interpreted in terms of magnetoacoustic waves (Edwin & Roberts 1983; Roberts, Edwin, & Benz 1984). Recently, transverse oscillations of active region loops have been observed with the *Transition Region and Coronal Explorer* (TRACE; e.g., Aschwanden et al. 1999; Schrijver & Brown 2000). These transverse loop oscillations are excited by flares, decay on a timescale on the order of 15 minutes, and have an oscillation period of roughly 5 minutes. The cause of the rapid damping has been a matter of considerable debate (Aschwanden et al. 1999; Nakariakov et al. 1999; Schrijver & Brown 2000; Ofman & Aschwanden 2002).

In order to study time variations and dynamics of active region loops, a number of spectral observations were made by the Solar Ultraviolet Measurement of Emitted Radiation (SUMER) spectrometer in recent *Solar and Heliospheric Observatory* (SOHO) campaigns. A preliminary investigation led to the discovery of several instances of Doppler shift oscillations in hot flare lines (e.g., Kliem et al. 2002; Wang et al. 2002). Here we report on a representative case that shows strong evidence that they are a manifestation of transverse loop oscillation excited impulsively.

### 2. OBSERVATION AND DATA REDUCTION

NOAA Active Region 9371 was observed by SUMER (Wilhelm et al. 1995) on 2001 March 9 at the west limb. The SUMER spectra were recorded on detector A with a 162 s exposure time and slit 1 ( $300'' \times 4''$ ) at a fixed position off the limb (see Fig. 1). The observations started at 09:55 UT and ended at 21:43 UT. The total data set consists of 23 groups of the spectral series. In each group, the first image has a spectral window of 1098–1138 Å, while the following 10 images use the left and right parts of this window alternately, with a small overlap containing the Ca X  $\lambda 557$  (in second order) and the Fe XIX  $\lambda 1118$  lines. The whole spectral window contains a number of lines formed in the temperature range of 0.01–10 MK. They include the relatively cool transition region line, S III/Si III  $\lambda 1113$  (0.03–0.06 MK), the coronal lines Ca X  $\lambda 557$  (0.7 MK) and Ca XIII  $\lambda 1133$  (2 MK), as well as the flare lines Fe XIX  $\lambda 1118$

(6.3 MK) and Fe XX  $\lambda 567$  (8 MK). The standard decomposition, corrections of flat field, detector distortions, dead time, and gain effects were applied to the raw data.

The data set contains two hot plasma events, exhibiting a sudden emission increase in the Fe XIX line and weak emission in Fe XX. The first event began at 15:49 UT, reached the maximum in intensity at 16:09 UT, and ended at about 16:40 UT. For the second event, the corresponding times are 17:31, 17:50, and 18:30 UT (see Fig. 2). Both events exhibit an oscillatory Doppler shift, as can be seen from Figure 2a, in which the spatial and temporal dependence of the wavelength shift, deduced from a Gaussian fit to the line profiles, is plotted.

During the periods of the SUMER events, the GOES X-ray satellite detected only a weak flare (identified to occur from another active region). The soft X-ray telescope (SXT) on *Yohkoh* obtained quiet-mode observations of AR 9371 in three time series around the SUMER events. The first SXT series from 14:51 to 15:53 UT, at the very beginning of the first SUMER event, did not show any flare brightenings occurring in the field of view ( $314'' \times 314''$ ). The second SXT series from 16:31 to 17:27 UT, just between the two SUMER events, revealed a weak loop appearing after the first event, whose top was close to the slit position where the SUMER event occurred. The third SXT series from 18:07 to 19:05 UT, covering the decaying phase of the second SUMER event, clearly showed a bright loop crossing the slit (see Fig. 1a), at a similar position to the earlier weak loop. Clearly, Fe XIX exhibits strong, sudden brightenings even in the absence of a flare.

TRACE observed AR 9371 in two EUV channels, one centered at 171 Å (observing Fe IX and Fe X, peak sensitivity at 1 MK), the other at 195 Å (Fe XII, 1.5 MK). The 171 Å images cover the duration from 12:01 to 17:56 UT, and the 195 Å images from 18:01 to 21:54 UT, each at a cadence of about 1 minute. The TRACE observations show many slowly evolving loops in AR 9371, some of which crossed the SUMER slit near the sites where the SUMER events took place, but there was no active or dynamic brightening before and during the SUMER events. It is worth noticing that the EUV loops are different in position and shape from the SXT loops (see Fig. 1).

### 3. RESULTS

Figure 2a shows the temporal evolution of the Fe XIX line shift. It reveals the two events, each of which exhibits two

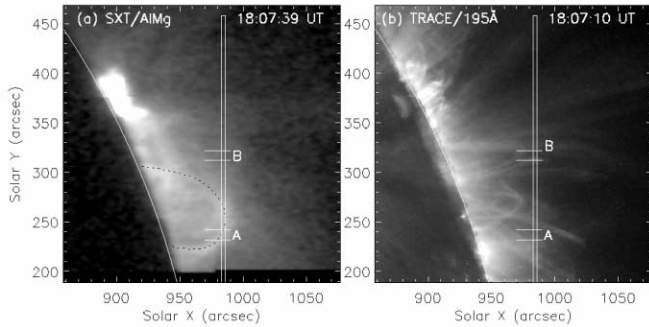


FIG. 1.—Near-simultaneous images made by (a) SXT and (b) TRACE at 195 Å. The SUMER slit position is indicated, and positions of two cuts (denoted A and B in Fig. 2a) are marked. The black dotted line in (a) outlines an SXT loop. Both images are plotted on a logarithmic brightness scale.

spatial components whose positions are the same for both events. For convenience, we call the first event “event 1” and the second “event 2,” while the lower and upper components are termed A and B. In both events, the lower and upper components oscillate in antiphase except at the start of event 1.

Figure 2b shows the spatially averaged shifts along the two strips marked A and B in Figure 2a. We fit the strongly damped oscillations by a function with five free parameters of the form

$$V(t) = V_0 + V_m \sin(\omega t + \phi)e^{-\lambda t}, \quad (1)$$

where  $V_0$  is the postevent Doppler shift,  $V_m$  is the oscillation amplitude, and  $\omega$ ,  $\phi$ , and  $\lambda$  are the frequency, phase, and decay rate of the oscillations, respectively. Then the oscillation period is given by  $P = 2\pi/\omega$ , the decay time is  $\tau_\lambda = 1/\lambda$ , and the displacement amplitude is  $A_m = V_m/(\omega^2 + \lambda^2)^{1/2}$  from the time integral of equation (1). The periods of the oscillations are 14–18 minutes, while the decay times are about 12–19 minutes. The periods of 1B and 2B are the same, while the periods of 1A and 2A differ from each other by about 4 minutes. The derived displacement amplitudes are  $A_m = 2000$ – $9400$  km.

The oscillations located at A and B are roughly in antiphase (i.e., phase difference  $\phi_A - \phi_B \approx \pi$ ). Figure 2b suggests that, particularly for the stronger A events, a damped sine wave does not represent the early evolution very well. The best fits put lower weighting on the initial data points for the A events. Events 1A, 2A, and 2B start with a large blueshift in the range of 62–77 km s<sup>-1</sup> that is about 2–3 times the maximum redshift.

Figures 2c and 2d show the evolution of the line intensity and shifts. Striking is the fact that the brightening and the velocity oscillations last for approximately the same time, ~30 minutes. The amplitudes of the brightening and of the line shift are not correlated, however. For example, the line intensity for B is much weaker than that for A, but their maximum shifts are quite similar (see Fig. 2d). The weaker intensity of B may be due to the fact that the slit position at B is farther away from the limb than at A, where the loop density and hence the emission are lower. The first (blueshifted) peak velocity is reached at or before the (first) brightness peak. We see that the lower and upper components (A and B) started simultaneously, strongly suggesting that they are generated by the same disturbing source or are correlated magnetically. Note that 1A is the only event for which the first blueshift is not the strongest. This first pulse is also out of phase with the remainder of the 1A oscillation (and in phase with the oscillation at 1B, which is inconsistent with the general antiphase rule between A and B). This weak initial Doppler peak of 1A coincides with a weak initial brightening and may be part of a separate event.

Consider now the spatial distribution along the slit of event A (Fig. 2). If we compare cuts A, C, and D (positions along the slit are marked in Fig. 2a), we notice that the oscillation remains in phase at all locations, with the exception of the first redshift, which starts earlier at positions A and D than at C. The diagonal feature at the lower part of 2A, marked by E (Fig. 2a), confuses the Doppler oscillation. It looks as though there is a strong blue-shift component moving northward at an apparent speed of about 23 km s<sup>-1</sup> (measured as the slope of cut E), which merges with the oscillation along 2D just before 18:00 UT. The evolutions of intensity and shift for cut E are also shown in Figures 2c and

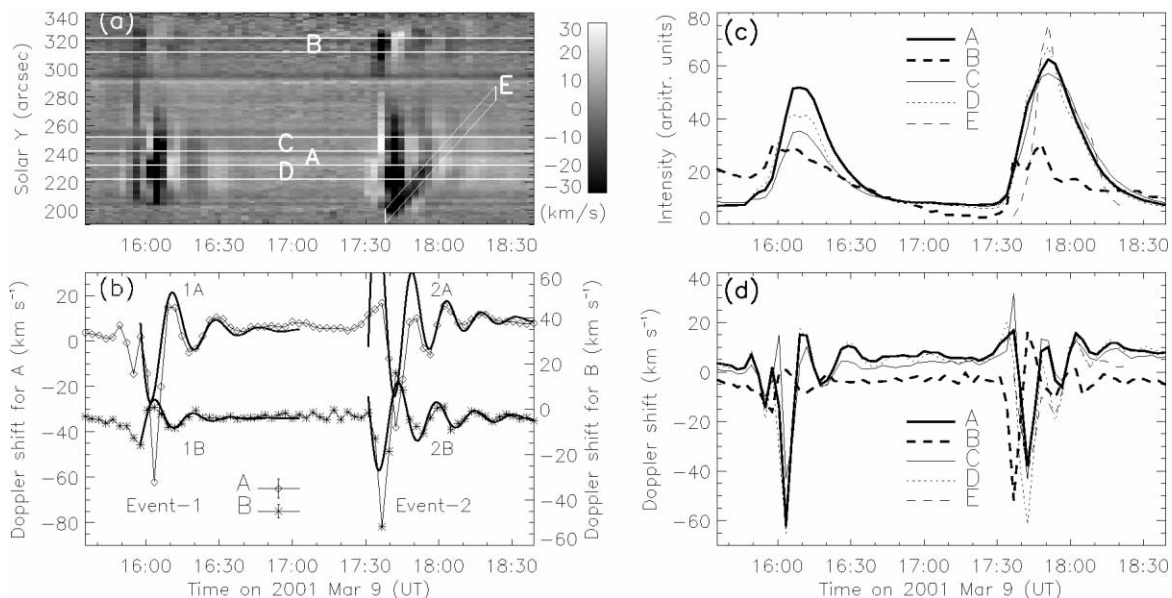


FIG. 2.—(a) Doppler shift time series at a fixed slit position (indicated in Fig. 1) in the Fe XIX line obtained by SUMER on 2001 March 9. The labels (A, B, C, D, and E) mark five strips with equal widths of 11 pixels along the slit. (b) Time profiles of Doppler shifts for A and B, averaged along the slit. The thick solid curves are the best fits employing function (1). (c) Average time profiles of line-integrated intensity for the five strips shown in Fig. 2a. For a clear comparison, the intensity in strip B has been stretched by a factor of 10. (d) Corresponding time profiles of Doppler shifts.

2d. The average Doppler shift is  $18 \pm 12 \text{ km s}^{-1}$  along this blueshift component during 17:37–17:56 UT.

It is likely that the southern component of the loop has moved northward, as suggested by E, because the bright SXT loop top cuts the SUMER slit at about  $15''$  north of cut A (Fig. 1a), where strong oscillations are seen at the start of the event. Nevertheless, we determine the parameters describing the loop geometry from the SXT image. We assume that the loop resembles a circular segment and that the midpoint between its footpoints is exactly above the limb. Then, from measurements of the footpoint separation and the apex position of the loop, we can determine the loop length, the inclination angle, and the azimuth angle using a method similar to that of Loughhead, Wang, & Blows (1983). For the analysis below the critical parameter is the loop length, which we determine to be 140 Mm.

#### 4. DISCUSSION

We analyze two similar flux enhancement events of the hot plasma observed in the SUMER spectra taken above AR 9371 when it was at the limb on 2001 March 9. Both events reveal strongly damped oscillatory Doppler shift profiles in the Fe XIX line, which last two or three periods, almost equal to the brightening duration. Each event consists of two spatial components of shifts oscillating almost in antiphase. The periods of the oscillations are 14–18 minutes, with a damping time or exponential decay time of 12–19 minutes. The events start with a strong blueshift with maximum velocities above  $60 \text{ km s}^{-1}$  and derived displacement amplitudes of 2000–9400 km. For comparison, the transverse oscillations of EUV coronal loops seen in TRACE 171 and 195 Å images show oscillation periods in the range of 2–11 minutes, decay times of 3–21 minutes, transverse amplitudes of 100–9000 km, maximum transverse speeds of 4–229  $\text{km s}^{-1}$ , and an average number of periods of  $4.0 \pm 1.8$  (over which the oscillation is visible; Schrijver, Aschwanden, & Title 2002; Aschwanden et al. 2002). So the SUMER Doppler oscillations have similar oscillation amplitudes, maximum speeds, and decay times, but there are two distinct differences. (1) The SUMER shift oscillations are observed only in hot plasma of more than 6 MK (e.g., a Ca X line formed at 0.7 MK or a Ca XIII line at 2 MK shows no oscillation), whereas the Fe IX  $\lambda 171$  and Fe XII  $\lambda 195$  lines are formed below 2 MK. (2) The oscillation periods in the SUMER observations are about 3 times longer than those in TRACE. We discuss these differences and interpret the SUMER shift oscillatory motions in the following paragraphs.

Flare lines like Fe XIX, Fe XX, and Fe XXI with formation temperature greater than 6 MK have been observed by SUMER above limb active regions in several flare events (Feldman et al. 1998, 2000; Innes et al. 2001; Kliem et al. 2002). In general, these flare lines show substantial Doppler broadening. Innes et al. (2001) revealed high-velocity blue- and redshifts in Fe XX preceded by bright, shifted emissions in several different temperature lines and showed evidence for a flare shock causing these features. Their spectral sequence did not make it possible to detect an oscillatory behavior of the shifts. Kliem et al. (2002) studied a case showing rapidly damped oscillatory Doppler shifts in Fe XXI correlated with oscillatory shifts of cool plasma in antiphase and interpreted these features in terms of reconnection outflows. Both these cases were associated with flares and coronal mass ejections (CMEs), while in our case, there was no associated GOES flare and no CME was seen in Large Angle and Spectrometric Coronagraph Experiment images. We did not find any signals in SUMER lines except the flare lines Fe XIX and Fe XX, consistent with the fact that no

erupting or dynamic EUV loops were seen in TRACE images during the Fe XIX events. Although the *Yohkoh* SXT observations did not cover the whole period of either SUMER event, a short overlap ( $\sim 4$  minutes) between the SXT and SUMER observations at the beginning of the first event showed no distinct flare features such as brightenings or X-ray ejecta occurring in the active region. However, it is possible that a flare-induced disturbance, coming from behind the limb, impacted on the coronal loops, causing their oscillations. We notice that the Fe XIX line is dominated by strong blueshifts at the onset of the events (Fig. 2b or 2d), and the SXT loops near the slit became brighter after the events (Fig. 1a), indicative of the above proposition.

We therefore interpret the oscillatory Doppler shifts in terms of (standing or propagating) waves in coronal loops triggered by an impulsive injection of energy at the start of the event. First, we find that the site where the oscillation component A occurred is very close to the top of an SXT loop that was brighter after the events, suggesting that this loop was related to the SUMER events. Second, the two SUMER events show similar features, such as periods, damping times, the presence of two components in antiphase, and a large initial blueshift. Also, they occur at the same spatial positions. All this strongly suggests that the magnetic topology was the same during the two events and thus argues against the interpretation of Kliem et al. (2002). This topology may consist of two magnetic loop systems; one was manifested as the SXT loop corresponding to the site of component A (Fig. 1a), while the other was manifested as a high EUV loop corresponding to component B (Fig. 1b). These two loop systems may have common footpoints behind the limb, likely related to a separatrix. This topology is similar to the one found by Wang, Wang, & Qiu (1999) for a disk active region, showing that two SXT loops repeatedly interacted at a common footpoint region, producing microflares. In such a topology, the two loops would move in opposite directions and the oscillations would be excited in antiphase if magnetic reconnection happens at the separatrix (Schrijver & Brown 2000). Schrijver, Aschwanden, & Title (2002) also found some cases of transverse oscillations of nearby loops in antiphase in TRACE EUV movies, and they suggested a similar explanation.

The loop oscillations observed by TRACE have been interpreted in terms of a kink mode standing wave (eigenmode), based on the good agreement with the observed periods (Aschwanden et al. 1999, 2002). We notice that the periods of Doppler shift oscillations of 14–18 minutes are evidently larger than the average period ( $5.4 \pm 2.3$  minutes) of transverse loop oscillations seen by TRACE. We find that all of the Doppler oscillations undergo an impulsive large blueshift at the flux rising phase of the events, significantly deviating from a damped sine function expected by the eigenmodes. This feature is in good agreement with the finding of Schrijver et al. (2002) and Aschwanden et al. (2002) that almost all of the oscillations start away from a triggering event (a flare or filament destabilization) and show an initial large displacement (Aschwanden et al. 2002). They argued that these features may indicate an impulsive excitation of loop oscillations in terms of propagating MHD waves rather than standing modes.

Next we attempt to identify the wave mode and to distinguish between standing and propagating waves. We first consider standing waves. In the active region corona, structures are expected to undergo three types of oscillations: the noncompressional kink waves and the compressional slow and fast magnetoacoustic waves (e.g., Roberts 2000). For a thin loop, only

the slow and kink modes exist. For a low- $\beta$  coronal plasma, where sound speeds ( $c_s$ ) are much smaller than Alfvén speeds ( $c_A$ ) inside the flux tube or loop, the slow magnetoacoustic speed  $c_t = c_s c_A / (c_s^2 + c_A^2)^{1/2} \approx c_s$  (Roberts et al. 1984), so the period of slow modes for a standing wave in its fundamental mode is

$$\tau_s = \frac{2L}{c_t} \approx \frac{2L}{c_s}, \quad (2)$$

where  $L$  is the length of the coronal loop and  $c_s = 117.7T^{1/2}$  m s<sup>-1</sup> ( $T$  is in units of kelvins). Taking  $L = 140$  Mm, measured from the SXT loop (Fig. 1a), and  $T = 6.3$  MK, the formation temperature of Fe XIX, we obtain  $c_s = 295$  km s<sup>-1</sup> and  $\tau_s \approx 15.8$  minutes. This agrees well with the measured period, but the absence of brightness fluctuations with the wave period (see Fig. 2c) argues against a compressible wave.

To estimate the period of the standing kink mode, we use an average coronal magnetic field of  $B \approx 30$  G and the upper limit of  $n_0 \approx 3.6 \times 10^9$  cm<sup>-3</sup> on the electron density inside the loop, from the RTV scaling law ( $n_9 = 0.13T_6^2/L_{10}$ ) for quasi-static loops (Rosner, Tucker, & Vaiana 1978), where  $n_9$  is in units of  $10^9$  cm<sup>-3</sup>,  $T_6 = 6.3$  in units of  $10^6$  K for the apex temperature, and  $L_{10} = 1.4$  in units of  $10^{10}$  cm. The period of the kink mode for a standing wave in its fundamental mode is given by Roberts et al. (1984) as follows:

$$\tau_k = \frac{2L}{c_k}, \quad c_k = c_A \left( \frac{2}{1 + n_e/n_0} \right)^{1/2}, \quad (3)$$

where  $n_e$  is the electron density outside the loop and  $c_A =$

$2.18 \times 10^{11} B n_0^{-1/2} \approx 1100$  km s<sup>-1</sup>. Assuming  $n_e/n_0 \sim 0.1$ , we obtain the phase speed of the kink mode of  $c_k \approx 1500$  km s<sup>-1</sup> and the period of  $\tau_k \approx 3.1$  minutes, which is 4 times lower than the period of the observed shift oscillation. For the period of the kink mode to match the observed period,  $\beta [ \equiv (2/\gamma)(c_s^2/c_A^2) ]$  for the hot coronal loop would have to be  $\sim 2$ , implying a 25 times greater density or 5 times weaker field.

Consider now propagating waves. If a disturbance is generated impulsively at one end of a loop, propagating MHD waves (all modes) will result (Roberts et al. 1984). Murawski, Aschwanden, & Smith (1998) point out that an initial pulse mainly excites the kink mode. Simulations (Murawski & Roberts 1994) have shown that the corresponding time profiles are complex, with a quasi-periodic behavior, a large initial peak, and rapid damping, which are all features of the observed evolutions. Their structure is therefore very similar to the observed oscillation; however, for the environment properties considered by Murawski & Roberts (1994) and Murawski et al. (1998), the oscillation period lies in the range of seconds, i.e., 1–2 orders of magnitude shorter than the periods deduced from SUMER observations. In our case, there is also no evidence of wave propagation along the SUMER slit, although it cannot be completely ruled out because the exposure time (2.7 minutes) was longer than the time for a kink wave to travel from the loop footpoint to apex,  $t_k = (L/2)/c_k \approx 47$  s. At present, we favor a standing wave as the cause of the observed oscillatory behavior detected by SUMER, although we cannot rule out propagating waves.

SUMER is a part of *SOHO* of ESA and NASA. *Yohkoh* is a mission of the Institute of Space and Astronautical Science (Japan), with participation from the US and UK. We thank Leon Ofman for his valuable comments.

#### REFERENCES

- Aschwanden, M. J. 1987, *Sol. Phys.*, 111, 113  
 Aschwanden, M. J., De Pontieu, B., Schrijver, C. J., & Title, A. 2002, *Sol. Phys.*, 206, 99  
 Aschwanden, M. J., Fletcher, L., Schrijver, C. J., & Alexander, D. 1999, *ApJ*, 520, 880  
 Berghmans, D., & Clette, F. 1999, *Sol. Phys.*, 186, 207  
 Edwin, P. M., & Roberts, B. 1983, *Sol. Phys.*, 88, 179  
 Feldman, U., Curdt, W., Doschek, G. A., Schuehle, U., Wilhelm, K., & Lemaire, P. 1998, *ApJ*, 503, 467  
 Feldman, U., Curdt, W., Landi, E., & Wilhelm, K. 2000, *ApJ*, 544, 508  
 Innes, D. E., Curdt, W., Schwenn, R., Solanki, S. K., & Stenborg, G. 2001, *ApJ*, 549, L249  
 Kliem, B., Dammasch, I. E., Curdt, W., & Wilhelm, K. 2002, *ApJ*, 568, L61  
 Loughhead, R. E., Wang, J.-L., & Blows, G. 1983, *ApJ*, 274, 883  
 Murawski, K., Aschwanden, M. J., & Smith, J. M. 1998, *Sol. Phys.*, 179, 313  
 Murawski, K., & Roberts, B. 1994, *Sol. Phys.*, 151, 305  
 Nakariakov, V. M., Ofman, L., DeLuca, E. E., Roberts, B., & Davila, J. M. 1999, *Science*, 285, 862  
 Ofman, L., & Aschwanden, M. J. 2002, *ApJ*, submitted  
 Roberts, B. 2000, *Sol. Phys.*, 193, 139  
 Roberts, B., Edwin, P. M., & Benz, A. O. 1984, *ApJ*, 279, 857  
 Rosner, R., Tucker, W. H., & Vaiana, G. S. 1978, *ApJ*, 220, 643  
 Schrijver, C. J., Aschwanden, M. J., & Title, A. M. 2002, *Sol. Phys.*, 206, 69  
 Schrijver, C. J., & Brown, D. S. 2000, *ApJ*, 537, L69  
 Wang, T. J., Solanki, S. K., Curdt, W., Innes, D. E., & Dammasch, I. E. 2002, in *Proc. 11th SOHO Workshop: From Solar Minimum to Maximum*, ed. A. Wilson (ESA SP-508; Noordwijk: ESA), in press  
 Wang, T., Wang, H., & Qiu, J. 1999, *A&A*, 342, 854  
 Wilhelm, K., et al. 1995, *Sol. Phys.*, 162, 189